JOURNAL OF OPTOELECTRONICS AND ADVANCED MATERIALS Vol. 9, No. 6, June 2007, p. 1699 - 1704

Structure and atomic transport properties in liquid AsTe alloys using AMEAM based potentials

S. SENTURK DALGIC*, S. SENGUL
Department of Physics, Trakya University, 22030 Edirne, Turkey

The static, dynamic structure and atomic transport properties of liquid AsTe alloys have been calculated using the integral equation theory with the effective pair potentials based on the analytic modified embedded atom method (AMEAM). The effective pair interactions are described with the potential functions recently proposed Hu and co-workers which are parametrized by fitting the cohesive energy, vacancy formation energy and equilibrium conditions of solid and liquid state properties of pure metals. In the structural calculations for liquid AsTe alloys, the thermodynamically self-consistent variational modified hypernetted chain (VMHNC) theory of liquids has been carried out to compute the partial static structure factors. The calculated single particle and collective dynamic properties have used to obtain the atomic transport properties, such as diffusion coefficients. The results have compared with available experimental data.

(Received November 14, 2006; accepted April 26, 2007)

Keywords: Liquid Arsenic-Tellurium Alloys, Structure, Analytic Modified Embedded Atom Method, Self-Diffusion Coefficient

1. Introduction

Liquid (l) As-chalcogenides, such as l-AsTe and l-AsSe, have covalently bonded network structures. These liquids have attracted considerable interest in both experimental and theoretical studies because they undergo the semiconductor to metal (SM) transition at high temperatures with increasing As concentration [1].Endo and co-workers have suggested from their EXAFS results that the metallic behaviour observed for liquid As-Te alloys at high temperature is governed by the bonding configuration of Te atoms [1]. Misawa has also shown that the experimentally obtained total structure factor for liquid $As_{20}Te_{80}$ was similar to the S(q) for liquid Te [2]. Maruyama *et.al.* have obtained the results of neutron diffraction (ND) experiments for l-AsTe alloys in the temperature range between 673K-873K and determined that the structural analysis of g(r) for liquid alloy containing 20 at.% As and 80 at. % Te gives the most reliable information on the partial correlation of Te, since the contribution of the pair correlation of AsAs is negligible [3].

On the other hand, theoretically the structure of the crystalline group-V elements has been discussed within the pseudopotential approach successfully [4]. Hafner has carried out the molecular dynamics calculations with l-As based effective pair interactions [5] and obtained results in good agreement with ND data. Shimojo et al. [6] have first studied the temperature dependence of atomic and electronic structures in the liquid As_2Te_3 by ab initio molecular dynamics simulations. Then arsenic chalcogen clusters have been studied with several researchers [7]. Popescu has proposed a closed cluster model for binary arsenic-chalcogen glasses and investigated the charge coordination defects in chalcogenide glasses [7].

It is well known that many body potentials based on the embedded atom method (EAM) or semi-empirical descriptions of atomic interactions have been used in many aspects of computer simulations and theoretical calculations. The embedded-atom method (EAM) which was originally proposed by Daw and Baskes (DB) [8] has been developed by several authors (References there in [9]). In the literature, there are several versions of EAM which are different with parameterisation methods and functions involved. Hu and co-workers [10] have proposed an analytic EAM potential (AEAM) for hcp metals. They added one another energy modification term, interpreted the anisotropy of hcp structure, in the total energy expression. Hu and co-workers have constructed a new analytic modified EAM (AMEAM) for hcp metals currently, and calculated the thermodynamic properties of Mg-Re alloys [11]. In our previous work, we have investigated the structural properties of liquid CdTe alloys with the AMEAM based potentials. To the best of our knowledge, there is no study of the AMEAM model for the liquid As-chalcogenides. In the present work, the potential functions of the AMEAM proposed by Hu and co-workers [10,12] have been used to obtain structural and atomic dynamic properties of l-As, l-Te and l-AsTe alloys. The effective interatomic potentials based on the AMEAM potential functions are constructed with the recently proposed Finnis-Sinclair (FS) type for the effective pair potential approximation of AMEAM [9] in our previous work. The constructed effective potentials are used as input data in our static and dynamic structure calculations. The partial structure factors and pair distribution functions are calculated with one of the integral equation theory of liquids namely, variational modified hypernetted chain (VMHNC) theory [13,14] which was successfully applied to metallic systems in the EAM calculations [15,16]. The VMHNC results are compared with available experimental data in order to determine the reliability of the AMEAM for describing the structural properties of liquid As, Te and AsTe systems. The self-diffusion coefficients for As and

Te at different alloy compositions have been also computed, and compared with the available results in literature.

2. Theory

2.1 Effective pair potentials

In the AMEAM, the basic equation of the total energy of a system of atoms is given by

$$E_{total} = \sum_i F(\rho_i) + \frac{1}{2}\sum_i \sum_{\substack{j \\ i \neq j}} \phi(r_{ij}) + \sum_i M(P_i) + \sum_i N(Q_i) \quad (1)$$

where the $F(\rho_i)$ is the embedding function, $\phi(r_{ij})$ is the pair potential between atoms i and j with distance r_{ij}, and ρ_i is the host electron density induced at site i by all other atoms in the system as

$$\rho_i = \sum_j f(r_{ij}) \quad (2)$$

where $f(r_{ij})$ is the only one electron density function. $M(P_i)$ and $N(Q_i)$ are the energy modification terms. The potential functions of AMEAM are same as in Refs.[9,10,12].

In order to construct the effective interatomic pair potential from the AMEAM, second and higher derivatives of the embedding function F are ignored. Recently proposed effective pair potential, $\phi_{eff}(r)$, form based on the Finnis–Sinclair (FS) approximation [17] with AMEAM are used. However, in this work, two different FS-AMEAM models have been used to calculate the effective pair potentials for liquid binary As-Te alloys. Model1 and Model2 are chosen to test of the applicability of different energy modification terms and electron density function. The model 1 is the same as given in Ref. [9]

$$\phi_{eff}^{AB}(r) = \phi_{AB}(r) - 2F'_{AB}(\rho)\left(M_{AB}(P_{AB}) + N_{AB}(Q_{AB})\right) f_{AB}(r) \quad (3)$$

where $F'(\rho)$ is the first derivative of the embedding function. The alloy pair potential $\phi_{AB}(r)$ between different atomic species, A and B type atoms in a binary alloy. For the Model 2; we note that the N(Q) terms taken as equal to zero in Eqs (1,3) as,

$$\phi_{eff}^{AB}(r) = \phi_{AB}(r) - 2F'_{AB}(\rho)\left(M_{AB}(P_{AB})\right) f_{AB}(r) \quad (4)$$

The all model parameters in Eqs.(3,4) are obtained by using the parameterization scheme given in Refs. [9,18].

2.2 The VMHNC Theory of Liquids

With the effective pair potential known, integral equations are able to provide us the liquid structure for metals and alloy. In our structural calculations, one of the integral equation theories which have shown to be very reliable theory of liquids VMHNC has been carried out [13-16]. Like most liquid state theories the VMHNC solves the Ornstein – Zernike (OZ) equation for binary system which defines the partial direct correlation functions, $c_{ij}(r)$, in terms of the total correlation functions $h_{ij}(r) = g_{ij}(r) - 1$, where $g_{ij}(r)$ denote the partial pair distribution functions. The OZ equation is supplemented by the exact closure relation. The partial static structure factor, $S_{ij}(q)$, for binary alloys can be written as Fourier transform of partial distribution functions:

$$S_{ij}(q) = \delta_{ij} + 4\pi(\rho_i \rho_j)^{1/2} \int \left(g_{ij}(r) - 1\right) \frac{\sin(qr)}{q} r dr . \quad (5)$$

The theoretical calculations can be compared with neutron or X-ray scattering experiments if the appropriate scattering parameters are known [3]. The total radial distribution for any concentration of alloy can be written by a linear combination of three partial pair distribution functions $g_{11}(r)$, $g_{12}(r)$ and $g_{22}(r)$.

2.3 The Dynamical Properties: Self Diffusion

Self diffusion constant is the important parameter for characterizing the liquid and as input into modelling heat and mass flow in crystal growth simulations. In order to compute the diffusion constant two different routes can be followed. First it can be defined as the Green-Kubo (GK) type equation in terms of the normalized velocity autocorrelation function Z(t) by

$$D = \frac{k_B T}{M} \int Z(t)\, dt \quad (6)$$

where M is the mass of atom. The second one is in terms of the mean square displacement, $\langle \Delta r^2(t) \rangle$, using the Einstein (E) relation as

$$D = \lim_{t \to \infty} \frac{\left\langle \Delta r^2(t) \right\rangle}{6t} . \quad (7)$$

In the present work, the diffusivity for each constituent in the alloy has been found using the theory for the dynamic structure calculations given in Refs. [19,20] for details.

3. Results and discussion

3.1. Pure Liquid Metals

First, we have calculated the effective pair potentials based on AMEAM potential functions for liquids As and Te at the thermodynamic states T=1103K; 0.04221 at./A^3 and T=1073K; 0.02617 at./A^3 , respectively. The input physical data used in our liquid state calculations determined from the solid sate values of Kittel [21] as

E_c^{liq}(eV):2.82 for As; 2.17 for Te; a^{liq}(A):3.45 for As; 4.05 for Te. All the parameters of potential functions are determined by not only fitting to solid but also liquid state properties using the parametrization procedure given in Ref. [9,18]. The model parameters for AMEAM used in our calculations are listed in Table 1.

Table 1. The parameters for l-As and l-Te used in AMEAM calculations.

Input parameters				Potential parameters		
Parameter		As	Te	Parameter	As	Te
Model 1	F_o(eV)	1.88	1.45	r_c (A)	5.14	5.13
	N	0.45	0.52	r_{1e} (A)	2.90	3.00
	α(eV)	0.5948	0.4867	k_{-1} (eV)	50.743	38.181
	β(eV)	-0.0064	-0.0813	k_0 (eV)	-223.196	-167.939
Model 2	F_o(eV)	1.88	1.45	k_1 (eV)	415.749	312.821
	N	0.74	0.84	k_2 (eV)	-427.738	-321.842
	α(eV)	0.3256	0.2085	k_3 (eV)	263.384	198.177
				k_4 (eV)	-97.207	-73.141
				k_5 (eV)	19.916	14.986
				k_6 (eV)	-1.747	-1.314

In Table 1, the r_c is the cut-off distance determined by the cut-off procedure [9,18]. The values of r_{1e} are determined from experimental pair distribution function as the position of the first peak. The number densities at these temperatures are evaluated by extrapolating of the empirical formula [22] which gives the temperature dependence of density for liquid metals and alloys linearly.

It has noted that the calculated effective pair potentials for liquids As and Te using AMEAM based Model1 and Model2 give the correct trend as far as the position of the concerned when compared with each other. The effective potential calculated by using Model1 gets deeper than the obtained from Model2 because of the contribution to energy of N(Q) term of the liquids. The presently obtained AMEAM effective pair potentials for As and Te are used as input data in our structural calculations. Calculated pair distribution functions for l-As and l-Te are shown in Figs.1a and 1b together with the neutron diffraction (ND) data of Bellisent *et.al.*[23] for l-As and Maruyama *et.al.* [3] for l-Te, respectively. It is shown that certain differences between calculated results and experiment, except first peak position of the g(r). In the case of l-Te, as shown in Fig. 1a, the calculated g(r) by using Model2 has a principal peak located at the same position and height of the experimental one. In contrast to the l-Te, the height of the calculated main peak of g(r) obtained by Model2 for l-As is underestimated. Also, the results of static structure factors have plotted with the neutron diffraction (ND) data. It is noticed that the calculated and experimental structure factors differ in depth of the first minimum. We also find that the oscillations in the calculated structure factors S(q) die out more rapidly than in the experimental data.

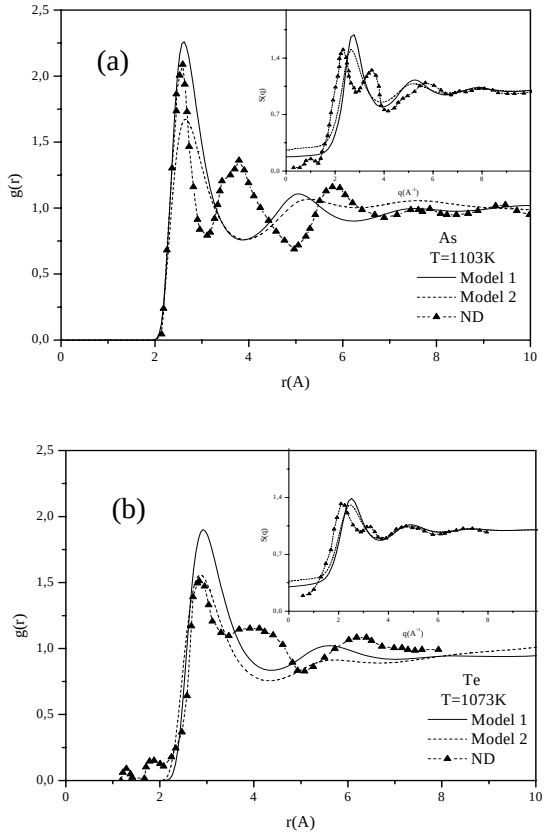

Fig. 1. The partial pair distribution functions for (a) l-As and (b) l-Te along with the experimental data of ND from Refs.[23,3], respectively. Insets show S(q)s'.

It is seen in Fig. 1 the results of S(q) using Model1 higher than those obtained by Model2. The calculated main peak is somewhat shifted to larger r values in comparison with the experiment. Especially for Te, it is observed a good agreement with the experiment in the large q values after that the second maxima.

3.2 Liquid Binary AsTe Alloys

For the liquid AsTe alloys, all calculations are performed at T=1073K, very near their melting. In Fig.2a, we have plotted the partial distribution functions, $g_{ij}(r)$, calculated by using Model2 for l-AsTe alloy at different concentrations. When it is decreased the concentration of Te in As_xTe_{1-x} alloys, it is appeared first peak height of $g_{ij}(r)$ gets close to that of l-Te (at 100%). The position of the main peak slightly shift to larger r values and the amplitudes of oscillation become radically different. We have also been displayed the partial structure factors for As-As, As-Te and Te-Te in equiatomic l-AsTe at 1073K calculated by using the AMEAM effective pair potentials with the VMHNC liquid state theory.

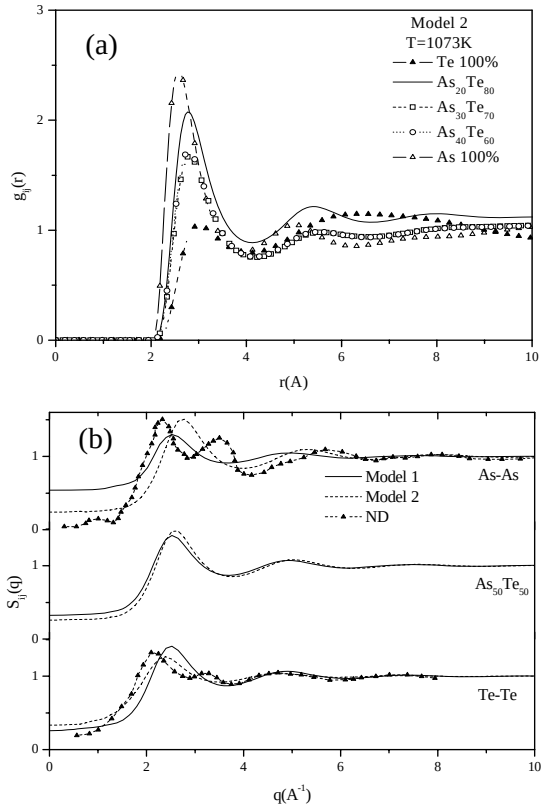

Fig.2. The calculated a) partial pair distribution functions and b) partial static structure factors for l-AsTe alloys.

We have plotted corresponding ND data of pure metals for the comparison; because of there are no theoretical and experimental results of the partial structure factor of l-AsTe.It is seen in Fig.2b that there are some discrepancies in low q-region. However, the calculated results of the $S_{ij}(q)$ are reasonable agreement with ND results at larger q region. The total pair correlation function, g(r), and total structure factor, S(q), for l-AsTe alloy at different concentrations are plotted in Figs 4a and 4b, respectively. For comparison, we have also included the ND data of Maruyama *et.al*[3]. The g(r) and S(q) were determined as a linear combination of corresponding partial ones. The values neutron scattering lengths needed to estimate total distribution function are 6.58fm and 5.8fm, respectively [24]. We find that the oscillations in our calculated g(r) die out more rapidly than in experimental ones. It is suggesting too soft repulsive potential. Qualitative similarity between total structure factor and ND data is fairly obvious. This shows that AsTe dimmers interact with the formation of TeTe bonds in molten AsTe.

3.3 Atomic Dynamical Properties

The self-diffusion coefficients, D, have been obtained from Eqs.(6,7) using these effective pair potentials and static structures. The calculated values of D for pure l-Te, l-As and l-$As_{20}Te_{80}$ alloy are listed in Table 2 along with the available experimental values. It is seen that both GK and E methods give consistent results with each other. D of l-Te is smaller than that of l-As because of the atomic size of Te is smaller than that of As. Especially, our calculated self diffusion from (E) and Model2 agree with theoretical and experimental values for l-Te and l-As.

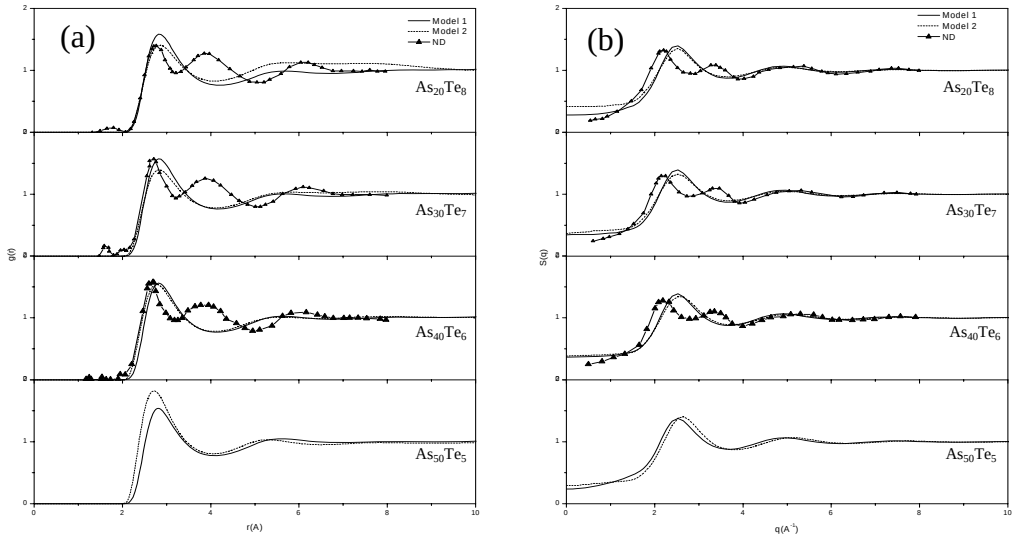

Fig. 3. The calculated a) total pair correlation functions and b) total structure factors using the AMEAM models for l-AsTe at 1073K. Temperatures of neutron diffraction data are 873K, 973K and 1073K for $As_{20}Te_{80}$, $As_{30}Te_{70}$ and $As_{40}Te_{60}$, respectively.

Table 2. The calculated self diffusion coefficients D.

	T(K)	D(A^2/ps)				
		Model 1		Model 2		Expt.
		GK	E	GK	E	
Te	1073	0.413	0.433	0.381	0.390	0.26[a]
As	1103	0.725	0.744	0.552	0.591	0.65[b]
		Self-diffusion from GK				
		Model 1		Model 2		
		As	Te	As	Te	
$As_{20}Te_{80}$	1073	0.731	0.410	0.521	0.378	
$As_{30}Te_{70}$	1073	0.741	0.402	0.533	0.394	
$As_{40}Te_{60}$	1073	0.748	0.422	0.539	0.401	
$As_{50}Te_{50}$	1073	0.754	0.427	0.547	0.415	

[a]from Ref[25] , [b]from Ref.[26]

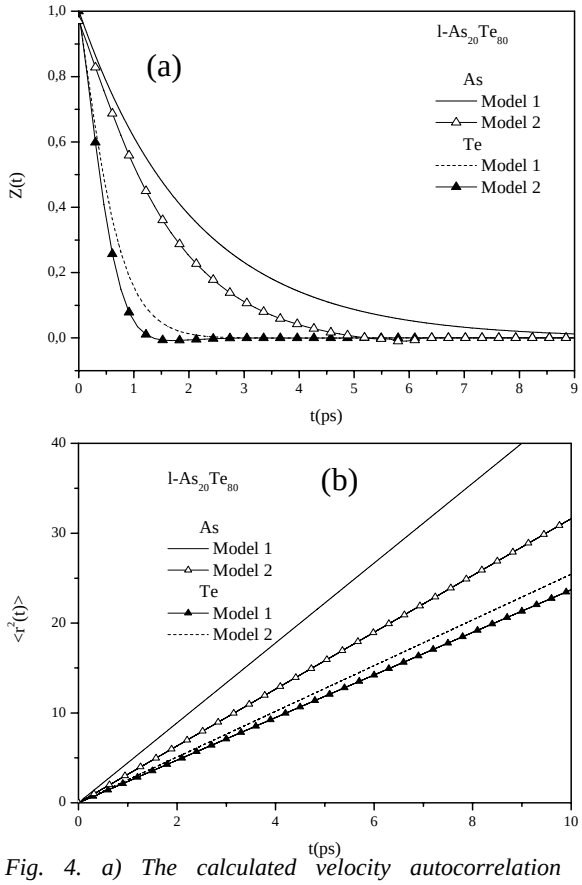

Fig. 4. a) The calculated velocity autocorrelation functions and b) mean square displacements for As and Te in l-$As_{20}Te80$ alloy.

There are no experimental and theoretical results for As_xTe_{1-x} alloys to compare with our calculations. It can be seen that the D coefficients of As and Te have increased by increasing the As concentration in $As_{20}Te_{80}$ alloys. The diffusion of As into the Te have been faster than that of Te into the As. In order to discuss time dependent properties of l-AsTe, the results of the normalized velocity autocorrelation function, Z(t), and mean square displacement, $\langle r^2(t)\rangle$, are plotted in Fig.4a,b for As and Te in l-$As_{20}Te_{80}$ alloy at 1073K, respectively. In all cases, except As from Model1, Z(t) becomes negative which is known as a famous cage effect due to temporary trapping of particles by their neighbours, and subsequently shows decay without any oscillations in contrast with the molten alkali and alkali-earth metals [20]. It is clearly relevant for the magnitude of D coefficient (proportional to the area under Z(t)) and it affects Z(t) in a short time regime. Fig. 4b, we it is possible to say, time dependence of $\langle r^2(t)\rangle$ shows typical behaviour for simple liquids at higher temperatures. For longer times, as soon as the motions become diffusive, the $\langle r^2(t)\rangle$ has a linear dependence on time

4. Conclusions

The improved functional form of the effective pair potential for AMEAM has been applied to liquid AsTe alloys. These calculations were performed with the potential functions that not only fit to solid data but also liquid state properties. The structural calculations were carried out using the VMHNC theory of liquids. Comparison between the results of the VMHNC theory and available experimental data show that the proposed AMEAM formalism for AsTe alloy systems is capable of providing a good description in their liquid state. However the discrepancies between the calculated results and experiment can be observed in intermediate q region. The calculated monatomic dynamical properties, such as self-diffusion, are consistent with available results in literature. The cage effects are seen in all cases, except l-As from Model1 because of its higher value of D. In the point of view, we have realized that AMEAM potentials can be apply to liquid As-chalcogenide systems in many aspects of computer simulations.

References

[1] H. Endo, H. Hoshino, H. Ikemoto, T. Miyanaga, J. Phys.:Condes. Matter. **12**, 6077 (2000).
[2] M. Misawa, J. Phys.:Condes. Matter. **4**, 9491 (1992).
[3] K. Maruyama, H. Hoshino, H. Ikemoto, H. Endo, J. Phys. Soc. Jpn **73** (2), 380 (2004).
[4] Y. Abe, I. Okoshi, A. Morita, J. Phys. Soc. Jpn. **42**, 504 (1977).
[5] J. Hafner, Phys. Rev. Lett. **62** (7), 784 (1989).
[6] F. Shimojo, S. Munejiri, K. Hoshino, Y. Zempo, J. Non-Cryst. Solids **312-314**, 349 (2002).
[7] M. Popescu, J. Optoelectron. Adv. Mater. **6**(4), 1147 (2004).

[8] M. S. Daw M. I. Baskes, Phys. Rev. **B29**, 6443 (1984); Phys. Rev. Lett. **50**, 1285 (1983).
[9] S. Senturk Dalgıc, S. Sengul, S. Kalaycı, J. Optoelectron. Adv. Mater. **7** (4), 2001 (2005).
[10] W. Hu, B. Zhang, B. Huang, F. Gao, D.J. Bacon, J. Phys.: Condens. Matter. **13**, 1193 (2001).
[11] W. Hu, H. Xu, X. Shu, X. Yuan, B. Gao, B. Zhang, J. Phys. D: Appl. Phys. **33**, 711 (2000).
[12] W. Hu, H. Deng, X. Yuan, M. Fukumoto, Eur. Phys. J. **B34**, 429 (2003).
[13] L. E. Gonzalez, A. Meyer, M. P. Iniguez, D. J. Gonzalez, M. Silbert, Phys. Rev **E47**, 4120 (1993).
[14] L. E. Gonzalez, D. J. Gonzalez, S. Dalgic and M. Silbert, Z. Phys. **B103,** 13 (1997).
[15] G. M. Bhuiyan, M. Silbert, M. J. Stott, Phys. Rev. **B 53**, 636 (1995).
[16] M. M. G. Alemany, C. Rey and L. J. Gallego, Phys. Rev. **B 58**, 685 (1998).
[17] M. W. Finnis, J. E. Sinclair, Phil. Mag. **A50**, 45 (1984).
[18] G. Tezgor, S. Senturk Dalgic, U. Domekeli, J. Optoelectron. Adv. Mater. **7** (4), 1983 (2005)
[19] M. M. Alemany, J. Casas, C. Rey, L.E. Gonzalez, L. J. Gallego, Phys. Rev. **E56** (6), 6818 (1997).
[20] S. Dalgic, M. Colakogullari, S. Senturk Dalgic, J. Optoelectron. Adv. Mater. **7** (4), 1993 (2005)
[21] C. Kittel, Introduction to Solid State Physics, 6th edition (1986).
[22] T. Iida, R.I.L. Guthrie, The Physical Properties of Liquid Metals (Clarendon Press, Oxford, 1993).
[23] R. Bellisent, C. Bergman, R. Ceolin, J.P. Gaspard, Phys. Rev. Lett. **59**, 661 (1987).
[24] V.F. Sears, Thermal-Neutron Scattering Lengths and Cross Sections For Condensed-Matter Research, Atomic Energy of Canada, Ltd. Report AECL-8490, June, 1984.
[25] D.H. Kurlat, C. Potard, P. Hicter, Phys. Chem. Liq. **4**, 183 (1974)
[26] X. P. Li, P.B. Allen, R. Car, M. Parrinello, J.Q. Broughton, Phys. Rev. **B41**(5), 3260 (1990).

*Corresponding auhor: se_sedat@yahoo.com